Pis'ma v ZhETF, vol. 93, iss. 3, pp. 139 – 143 © 2011 February 10

Extremely slow intramolecular vibrational redistribution: Direct observation by time-resolved Raman spectroscopy in trifluoropropyne

A. L. Malinovsky[+], *A. A. Makarov*[+*1)], *E. A. Ryabov*[+]

[+]*Institute of Spectroscopy RAS, 142190 Troitsk, Moscow Region, Russia*

[*]*Moscow Institute of Physics and Technology, 141700 Dolgoprudny, Moscow Region, Russia*

Submitted 21 December 2010

We have studied the dynamics of intramolecular vibrational redistribution (IVR) from the initially excited mode $\nu_1 \approx 3330\,\mathrm{cm}^{-1}$ (acetylene-type H–C bond) in H–C≡C–CF_3 molecules in the gaseous phase by means of anti-Stokes spontaneous Raman scattering. The time constant of this process is estimated as 2.3 ns – this is the slowest IVR time reported so far for the room-temperature gases. It is suggested that so long IVR time with respect to the other propyne derivatives can be explained by a larger defect, in this case, of the Fermi resonance of ν_1 with $\nu_2 + 2\nu_7$ – the most probable doorway state leading to IVR from ν_1 to the bath of all vibrational – rotational states with the close energies. In addition, it is shown that the observed dynamics is in agreement with a theoretical model assuming strong vibrational – rotational mixing.

Intramolecular vibrational energy redistribution (IVR) is a subject of fundamental importance for such areas as foundations of statistical theories of unimolecular reactions, dynamical chaos in polyatomic molecules, mode-selective laser-induced chemistry, and others (for review, see Refs. [1 – 6]). In mode selective chemistry, IVR is of practical importance – to achieve selectivity, one needs to pump energy into a specific vibrational mode faster than the relaxation of this energy to other modes of the molecule occurs. In spectroscopy, IVR manifests itself in the relaxation of the initially prepared "Zero Order Bright State" ($|\mathrm{ZOBS}\rangle$ [5]), which is usually a fundamental or an overtone excitation of a specific vibrational mode of the molecule, into a manifold of other states with almost the same total energy, but in which energy is divided among many degrees of freedom of the molecule.

The IVR time-scales, depending on the molecule and the total energy in the system, usually range from hundreds of femtoseconds (e.g., benzene CH overtones [7, 8]) to hundreds of picoseconds (e.g., terminal acetylene fundamental $\nu_1 \equiv \nu_{\mathrm{HC}}$ in butyne and pentyne [9]). Even more, in Ref. [10] by Quack et al., observation of some nanosecond relaxation process in CF_3I was reported. Also, nanosecond IVR times τ_{IVR} were extracted from high-resolution spectra of the terminal acetylene mode ν_1 of two molecules: HC≡CSi$(CH_3)_3$ ($\tau_{\mathrm{IVR}} \approx 2$ ns) HC≡CSn$(CH_3)_3$ ($\tau_{\mathrm{IVR}} \approx 6$ ns) [11].

Two latter examples as well as the example of Ref. [9] relate to spectroscopy in the cold molecular beams (CMB) [3]. More recent real time experiments with the room-temperature gases (RTG) showed much shorter IVR times in the same terminal acetylene molecules. The $|0\rangle \to |1\rangle$ transition in the mode $\nu_1 \approx 3330\,\mathrm{cm}^{-1}$ was pumped by a short laser pulse. Then, to measure depopulation of the state $|1\rangle \equiv |\mathrm{ZOBS}\rangle$ due to IVR, two different probe methods were used: the infrared (IR) absorption at the $|1\rangle \to |2\rangle$ transition, and anti-Stokes Raman scattering (RS) at the $|1\rangle \to |0\rangle$ transition. So, in the case of HC≡CSi$(CH_3)_3$, the IVR time $\tau_{\mathrm{IVR}} \approx 96$ ps was obtained by the IR probe [12], and $\tau_{\mathrm{IVR}} \approx 128$ ps – by the RS probe [13].

Moreover, for two molecules, propyne HC≡CCH_3, and propargyl chloride HC≡CCH_2Cl, the IVR effect was not observed in the CMB studies at all, but it was clearly seen in the RTG studies [12, 14, 15]. For quantitative treatment of this difference, we suggested a theoretical model [14 – 16] assuming that all (close to ν_1) vibrational – rotational states with the same total angular momentum J and full vibrational – rotational symmetry participate in IVR, regardless of the rotator quantum number K (in the case of HC≡CCH_3), or K_a (in the case of HC≡CCH_2Cl), and the vibrational quantum numbers as well. In the other words:

- projection K of the total angular momentum J on the symmetry axis of propyne, and its analog K_a in the case of propargyl chloride cease to be "good" quantum numbers in the bath of vibrational – rotational states[2)];

[1)] e-mail: amakarov@isan.troitsk.ru

[2)] Nonconservation of K_a was also observed in high-resolution spectra of ethanol [17], propargyl amine [18], and propargyl alcohol [19].

- this effect takes place, at least, as low as the energy of ν_1 is reached;
- implying "strong" mixing of zero-order states in the bath (with conservation of only the total angular momentum J and full vibrational–rotational symmetry), this effect can be explained by that mixing is mediated by not only anharmonic interactions, but also vibrational–rotational ones;
- then the difference between CMB and RTG experimental results can be naturally referred to as due to a gain of vibrational–rotational interactions for higher rotational quantum numbers engaged at room temperature.

An object to study in the present work is trifluoropropyne $HC{\equiv}CCF_3$. Only few perturbations (but no IVR) were earlier observed in the spectrum of ν_1 fundamental in the CMB study of Ref. [20]. In our real time RTG experiment, IVR is clearly seen, however.

The experiment details are as follows. The Nd^{3+}:YAG laser with a pulse duration of 37 ps (FWHM) was used both for the pumping of the $LiNbO_3$ optical parametric oscillator (OPO) and for the RS probing purposes. The pump pulse from OPO (20 ps) and probe pulse were aligned coaxially and focused into the gas cell. The pump beam spot profile was about 200 μm in diameter, while the waist diameter of the probe beam was approximately twice narrower. The polarizations of these two beams were perpendicular to each other. The pump pulse energy amounted to 200–300 μJ. The probe pulse energy was naturally limited by multiphoton effects occurring in the strong laser field and leading to visible luminescence. In our experiments, this energy did not exceed 5 mJ. The delay time between the pump and probe pulses was adjusted by means of a mechanically movable prism. The zero delay time between the pulses was established from the maximum of the signal at the sum frequency $\omega_{\rm OPO} + 2\omega_{\rm YAG}$ that was generated upon upconversion in a $LiIO_3$ crystal. The accuracy of such a tie-in was ± 3.3 ps. The pulse repetition rate was equal to 12.5 Hz. The OPO wavelength in the 3 μm region was tuned in to the ν_1 band of the $HC{\equiv}CCF_3$ molecule. The OPO radiation spectrum, whose width was approximately 50 $\rm cm^{-1}$ (FWHM), covered completely the whole ν_1 rotational structure. The RS signal was detected using a triple polychromator in the range 785.7–788.1 nm that covered the anti-Stokes position of the ν_1 band. It was registered in a photon counting mode by means of a Hamamatsu H7421-50 unit and a SR400 gated pulse counter.

The experimental data are shown in Fig.1 for two gas pressures, 6 and 30 Torr, with the corresponding experimental errors. The theoretical modeling, represented by solid and dashed curves in Fig.1, starts from that the 6 Torr data are treated, in zero approximation, as pure IVR without any collision-induced process. Then the IVR rate W_0 is roughly estimated by the one-exponential fitting the data shown in Fig.1a.[3)] This IVR rate W_0 is used to evaluate the so-called dilution factor σ, i.e. the level of the RS signal that should be at the delay times $\tau_{\rm d} \gg W^{-1}$. Such evaluation is possible due to that the pair of two quantities $\{W, \sigma\}$ defines the value of $\rho_{\rm eff}$ of those bath states $|b\rangle$, interaction of which with the state $|1\rangle$ leads to IVR. Correlation of three quantities above (W, σ, and ρ) can be understood, e.g., in terms of the Bixon–Jortner model [21], where one state

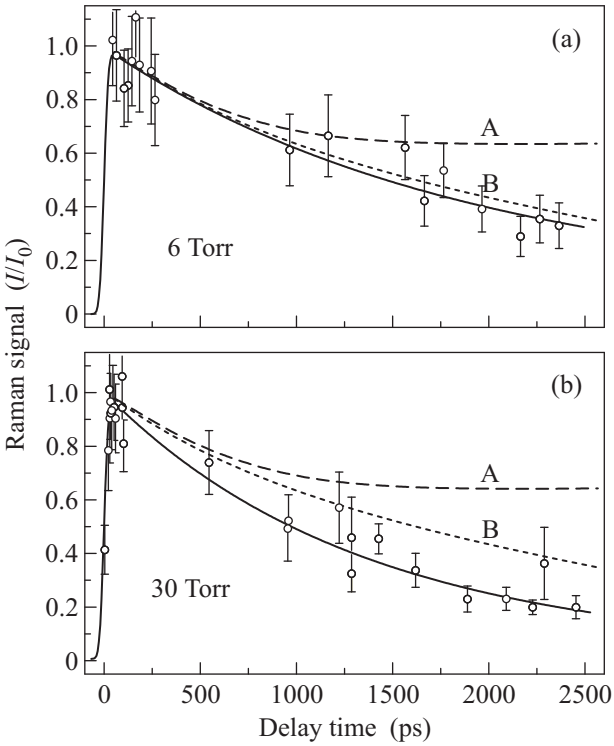

Fig.1. Anti-Stokes Raman signal in the ν_1 band of trifluoropropyne (in units of I_0 defined as a signal intensity at zero delay time and a vanishingly short excitation pulse) vs the pump–probe delay time. Results are presented for two pressures. The measurement error is determined by the statistics of photon counts. The pair of solid curves in (a) and (b) presents the best simultaneous fit using Eq. (1). The dashed curves show what would be at scenarios A (upper) and B (lower) with the same IVR rate

[3)] Procedure of fitting always includes double convolution of a decay function with the pump and probe pulse shapes.

(denoted as $|1\rangle$, or $|\mathrm{ZOBS}\rangle$ in our consideration) uniformly interacts with an infinite set of equidistant states $|b_i\rangle$ with an energy spacing ρ^{-1}. Herein, the value of the quantity $W = 2\pi|V_{1b}|^2\rho$ gives an estimate for the rate of depopulation of the state $|1\rangle$, and the value of the quantity ρ^{-1} defines the recurrence time. Competition between depopulation and recurrence supports the mean population $\mathcal{P}(t)$ of the state $|1\rangle$ at long times, what is equivalent to the dilution factor σ.

In reality, to describe the experiments under discussion (RTG – Raman), the Bixon – Jortner model should be generalized in two directions. The reasons are the following: (i) the interaction matrix element V_{1b_i} fluctuates, and so does the spacing between adjacent states $|b_i\rangle$; (ii) initial states, denoted as $|1\rangle$, belong to an ensemble of thermally populated vibrational – rotational states where exactly one quantum is added into mode ν_1, so that the value of ρ depends on the quantum numbers of a given state $|1\rangle$. Hence, the experimentally observed values of W and σ should be treated as ensemble-averaged ones, and any relevant theoretical model must include averaging procedures that take into account the remarks (i) and (ii) above.

The first task (i) can be solved numerically with an assumption about the statistics of the matrix elements and spacings. Results of such calculations were presented in Ref. [15] for chaotic statistics (modeled by the Gaussian orthogonal ensemble [22, 23]) as a family of curves $\mathcal{P}_\varkappa(t)$ depending on the parameter $\varkappa = W\rho$. The solution of the second task (ii) is based on direct calculations of ρ for any initial state followed by averaging over the Boltzmann vibrational – rotational ensemble for a given temperature.

For the results presented in Fig.1, a scenario has been investigated, first, with an assumption that ρ_{eff} is the density of *vibrational* states, ρ_{vib}, of the same symmetry as that of the initial state (scenario A). The calculation procedure includes averaging over all initially populated vibrational states, and the obtained value of the dilution factor is $\sigma \approx 0.67$. As can be seen from Fig. 1a, this value is far from reality. So, secondly, scenario B has been accepted where ρ_{eff} is the density of *all* vibrational – rotational states $\rho_{\mathrm{vib-rot}}$, with conservation of only the total angular momentum J and full vibrational – rotational symmetry. Here, the obtained value of the dilution factor proves to be $\sigma \approx 0.12$ that does not contradict to the data of Fig.1. An information on densities of states is summarized in Table1. State densities (in states/cm^{-1}) are calculated within the harmonic approximation using a window of $\pm 5\,\mathrm{cm}^{-1}$. The vibrational frequencies from Ref. [24] are used, and the rotational constants are from Ref. [25]. The angle brackets mean averaging over Boltzmann distribution at a temperature of 293 K, and N_0 is the corresponding population of the ground state.

Table 1

Characteristics of trifluoroprpopyne

N_0	ρ_{vib} [a)]	$\langle\rho_{\mathrm{vib}}\rangle$	$\langle\rho_{\mathrm{vib-rot}}\rangle$
0.19	9.5	60	5800

[a)] Density of vibrational states of symmetry A_1 at an energy of 3330 cm^{-1}, i.e. near the state with one quantum in the mode ν_1 and zero in all other modes.

With the latter value of the dilution factor σ, the next-order two-exponential fit is applied to the data in Fig.1 for the both pressures. This procedure takes into account depopulation of the state $|1\rangle$ due to collisions. Then the following formula is used:

$$\mathcal{P} = (1-\sigma)\exp\left[-\left(\frac{W}{1-\sigma} + kp\right)\tau_{\mathrm{d}}\right] + \sigma\exp(-kp\tau_{\mathrm{d}}), \tag{1}$$

where $\mathcal{P}(\tau_{\mathrm{d}})$ is the decay function normalized by condition $\mathcal{P}(0) = 1$, p is the gas pressure, k is the rate constant of collision-induced IVR [26], and the value of W is divided by $(1-\sigma)$ in the first exponential function to guarantee that $d\mathcal{P}/d\tau_{\mathrm{d}} \equiv -W$, at $\tau_{\mathrm{d}} = 0$ and $p \to 0$, has really a sense of IVR rate. Our final evaluation of all parameters entering Eq. (1) is: $\tau_{\mathrm{IVR}} \equiv W^{-1} = 2.3 \pm 0.3$ ns, $\sigma = 0.12 \pm 0.01$, $k = 10.1 \pm 1.2\,\mu\mathrm{s}^{-1}\cdot\mathrm{Torr}^{-1}$.

So, the slowest IVR rate is observed, in the case of trifluoropropyne, for room-temperature conditions. It is about 6.6 times smaller than that in the case of propyne [15], and about 2.2 times smaller than that in the case of propargyl chloride [14, 15]. We suggest a likely explanation of this difference assuming that, for ν_1, the main doorway state in the first tier of the well known IVR scheme[4)] (see Fig.2) is the combination $\nu_2 + 2\nu_7 \approx 3537\,\mathrm{cm}^{-1}$. This choice is natural, since $\nu_2 \approx 2165$ cm^{-1} corresponds to the C≡C stretch vibration, and $\nu_7 \approx 686$ cm^{-1} corresponds to the H–C≡C bend vibration, both being spatially the closest modes to ν_1. We don't consider additional details, only assuming the most general couplings of the doorway state to the bath states by a chain of anharmonic and vibrational–rotational interactions. In the case of one dominating doorway state $|\mathrm{DWS}\rangle$, the formula for the IVR rate from

[4)] The tier model was applied to terminal acetylene molecules in Ref. [27] (see also references therein). The combination $\nu_{\mathrm{C\equiv C}} + 2\nu_{\mathrm{H-C\equiv C}}$ was considered as a dominating doorway state in Ref. [28], and also mentioned as a possible candidate in Ref. [9] (fig.7b, and the acompanying text), and Ref. [12] (Appendix A).

Table 2

Characteristics of combination state $\nu_{C\equiv C} + 2\nu_{H-C\equiv C}$ in propyne, propargyl chloride, and trifluoropropyne (in cm^{-1}), and corresponding IVR times (in nanoseconds)

Molecule	$\nu_{C\equiv C} + 2\nu_{H-C\equiv C}$			ΔE		W^{-1} (ns)
	Assignment	Harmonic	Observed	Harmonic	Observed	
$HC\equiv CCH_3$	$\nu_3 + 2\nu_9$	3408	3381 [a]	-74	-47	0.35 [b]
$HC\equiv CCH_2Cl$	$\nu_3 + 2\nu_8$	3447	(?)	-112	(?)	1.05 [b]
	$\nu_3 + 2\nu_{14}$	3421	(?)	-86	(?)	
$HC\equiv CCF_3$	$\nu_2 + 2\nu_7$	3537	~ 3500 [c] (?)	-207	-170	2.3 [d]

[a] See Ref. [29] for spectral measurements of $\nu_3 + 2\nu_9$. In addition, the value of anharmonic coupling of this combination state to ν_1 (i.e. $\langle ZOBS|\widehat{V}_{anh}|DWS\rangle$ in our model) has been estimated from the band intensity as 7 cm^{-1} (cf. with our estimate in the text).
[b] From Ref. [15].
[c] Only a "very weak" band ranging from 3492 to 3505 cm^{-1} and centered at 3501 cm^{-1} has been observed in the region where $\nu_2 + 2\nu_7$ may be expected [24]. It has been assigned as $\nu_1 + \nu_{10}$ (the low frequency bend C≡C–C vibration), but it is very probable that it is just $\nu_2 + 2\nu_7$, at least in a considerable part.
[d] This work.

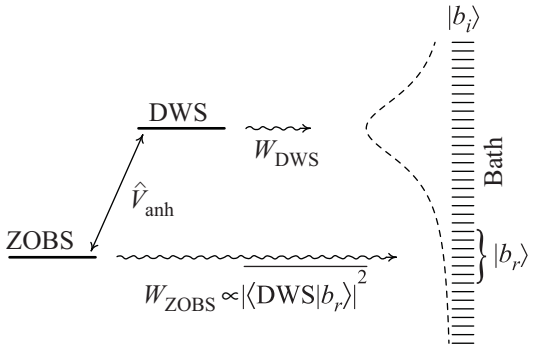

Fig.2. IVR from the Zero Order Bright State $|ZOBS\rangle$ into the bath of dark vibrational–rotational states $|b_i\rangle$ in a case where one doorway state $|DWS\rangle$ dominates. The IVR rate W_{ZOBS} is proportional to the squared projection of DWS onto $|b_r\rangle$ – those bath states that are approximately resonant to $|ZOBS\rangle$. The quantity $|\langle|DWS|b_i\rangle|^2$ is distributed, on average, as a Lorentzian of the width equal to the rate of IVR from $|DWS\rangle$, as schematically shown by the dashed curve

state $|ZOBS\rangle$ can be given in terms of the following quantities: the *energy defect* $\Delta E = \nu_{ZOBS} - \nu_{DWS}$ of the corresponding Fermi resonance, the nondiagonal matrix element of the anharmonic interaction $\langle ZOBS|\widehat{V}_{anh}|DWS\rangle$, and the rate W_{DWS} of IVR from the doorway state. In particular, at conditions $\langle ZOBS|\widehat{V}_{anh}|DWS\rangle \ll \Delta E$ and $W_{DWS} \ll \Delta E$, the rate of IVR from the state $|ZOBS\rangle$ is

$$W_{ZOBS} \approx \left(\frac{\langle ZOBS|\widehat{V}_{anh}|DWS\rangle}{\Delta E}\right)^2 W_{DWS}\,. \qquad (2)$$

In our case, $\Delta E = \nu_1 - \nu_2 - 2\nu_7 \approx -207\,cm^{-1}$ (in the harmonic approximation), and the term $q_1 q_2 (q_{7x}^2 + q_{7y}^2)$ in the expansion of potential energy in the normal coordinates q_i plays the principal role[5]. To satisfy the experimentally measured IVR rate in our experiment, one may set in Eq. (2), e.g., $\langle ZOBS|\widehat{V}_{anh}|DWS\rangle = 5 - 10\,cm^{-1}$ and $W_{DWS}^{-1} = 1.3 - 5.2$ ps, respectively. These both estimates are rather realistic.

Let us consider now the physically same combinations in the cases of propyne and propargyl chloride. Available data are summarized in Table 2. One can see that the corresponding energy defects ΔE increase in the raw together with the IVR time. Surely, it is only a qualitative treatment, pretending just to that the combination $\nu_{C\equiv C} + 2\nu_{H-C\equiv C}$ *might be* a doorway state playing a major role in IVR from ν_{H-C} for the terminal acetylene molecules $H-C\equiv C-X$ with different X. Let us look, nevertheless, at what should be with the doorway-state IVR rates if the value of coupling $\langle ZOBS|\widehat{V}_{anh}|DWS\rangle$ is taken equal for all three molecules with the value given in Table 2 (footnote a). Using Eq. (2), the values of ΔE from the last column of Table 2 for propyne and trifluoropropyne, and experimentally measured values of W_{ZOBS} one gets $W_{DWS}^{-1} \approx 7.8$ ps (propyne), and $W_{DWS}^{-1} \approx 3.9$ ps (trifluoropropyne). For propargyl chloride (that is intermediate between previous examples as far as concerned the state density), we have only harmonic values of ΔE. Using them and dividing the coupling squared equally between two doorway states one gets $W_{DWS}^{-1} \approx 5.5$ ps. Qualitatively, the noticed increase (from molecule to molecule) in the "intra-bath" IVR rate can be interpreted as due to reduction in the number of high-frequency modes and consequent increase in the density of intermode resonances, at least, of the 3-rd and 4-th orders. This quantity plays the key role in

[5] Since the mode ν_7 is two-fold degenerate, then only the symmetric component of the $q_{7j}q_{7k}$ tensor ($j,k \leftrightarrow x$ or y) enters $\widehat{V}_{anh}$.

the transition to chaotic dynamics [30 – 33], and enters the IVR rate as well [34 – 36]. In addition, it shoud be noted that an estimated value of several picoseconds for the intra-bath IVR time scale may be rather typical for a medium-size "compact" molecule, as, e.g., $(CF_3)_2CCO$ studied recently in Ref. [37].

So, the results of the presented study are:

1. A time of 2.3 ns is measured for the IVR from the first excited state of the acetylene- type H – C mode of $HC{\equiv}CCF_3$. This time is several times slower than that for the other terminal acetylene molecules at the same room-temperature conditions. We suggest a natural explanation of this difference.

2. A rate of $10.1\,\mu s^{-1}Torr^{-1}$ (corresponding to a few gas-kinetic collisions) is measured for the collision-induced IVR from the same state. This rate is approximately the same as in the case of $HC{\equiv}CCH_2Cl$ ($8.5\,\mu s^{-1}{\cdot}Torr^{-1}$; see Ref. [14]).

3. Experimental results are inconsistent with an assumption that IVR in $HC{\equiv}CCF_3$ occurs as an exchange of only the vibrational quanta, but are consistent with that the strong vibrational – rotational mixing is present.

This work was supported by the Russian Foundation for Basic Research (grant # 09 – 02 – 00495-a).

1. *Laser Spectroscopy of Highly Vibrationally Excited Molecules*, Eds. V. S. Letokhov, Adam Hilger, Bristol, 1989; M.: Nauka, 1990 (in Russian).
2. T. Uzer, Phys. Rep. **199**, 73 (1991).
3. K. K. Lehmann, G. Scoles, and B. H. Pate, Annu. Rev. Phys. Chem. **45**, 241 (1994).
4. P. M. Felker and A. H. Zewail, *Jet Spectroscopy and Molecular Dynamics*, Eds. J. M. Hollas and D. Phillips, Blackie, London, 1995, p. 222.
5. D. J. Nesbitt and R. W. Field, J. Phys. Chem. **100**, 12735 (1996).
6. M. Gruebele, in: *Advances in Chemical Physics*, Eds. I. Prigogine and S. A. Rice, John Wiley & Sons, New York, 2000, Vol. **114**, p. 193.
7. K. V. Reddy, D. F. Heller, and M. J. Berry, J. Chem. Phys. **76**, 2814 (1982).
8. R. H. Page, Y. T. Lee, and Y. R. Shen, Phys. Rev. Lett. **59**, 1293 (1987).
9. A. Mcllroy and D. J. Nesbitt, J. Chem. Phys. **92**, 2229 (1990).
10. M. Quack, R. Schwarz, and G. Seyfang, J. Chem. Phys. **96**, 8727 (1992).
11. E. R. Th. Kerstel, K. K. Lehmann, T. F. Mentel et al., J. Phys. Chem. **95**, 8282 (1991).
12. H. S. Yoo, M. J. DeWitt, and B. H. Pate, J. Phys. Chem. A **108**, 1348 (2004).
13. A. L. Malinovsky, A. A. Makarov, and E. A. Ryabov, Pis'ma v ZhETF **80**, 605 (2004); JETP Lett. **80**, 532 (2004).
14. A. L. Malinovsky, Yu. S. Doljikov, A. A. Makarov et al., Chem. Phys. Lett. **419**, 511 (2006).
15. A. L. Malinovsky, A. A. Makarov, and E. A. Ryabov, ZhETF **133**, 45 (2006); JETP **106**, 34 (2008).
16. A. A. Makarov, A. L. Malinovsky, and E. A. Ryabov, J. Chem. Phys. **129**, 116102 (2008).
17. J. S. Go, G. A. Bethardy, and D. S. Perry, J. Phys. Chem. **94**, 6153 (1990).
18. A. M. Andrews, G. T. Fraser, and B. H. Pate, J. Chem. Phys. **109**, 4290 (1998).
19. E. Hudspeth, D. A. McWhorter, and B. H. Pate, J. Chem. Phys. **109**, 4316 (1998).
20. B. H. Pate, K. K. Lehmann, and G. Scoles, J. Chem. Phys. **95**, 3891 (1991).
21. M. Bixon and J. Jortner, J. Chem. Phys. **48**, 715 (1968).
22. A. Bohr and B. R. Mottelson, *Nuclear Structure*, Benjamin, New York, 1969, Vol. 1, Ch. 2, Appendix 3.
23. E. Ott, *Chaos in dynamical systems*, Cambridge University Press, Cambridge, 1993, p. 334.
24. C. V. Berney, L. R. Cousins, and F. A. Miller, Spectrochim. Acta **19**, 2019 (1963).
25. J. N. Shoolery, R. G. Shulman, W. F. Sheehan et al., J. Chem. Phys. **19**, 1364 (1951).
26. A. A. Kosterev, A. A. Makarov, A. L. Malinovsky, and E. A. Ryabov, Chem. Phys. **219**, 305 (1997).
27. A. A. Stuchebrukhov and R. A. Marcus, J. Chem. Phys. **98**, 6044 (1993).
28. A. L. Malinovsky, A. A. Makarov, and E. A. Ryabov, Proc. SPIE **6580**, 65800K (2006).
29. E. R. Th. Kerstel, K. K. Lehmann, B. H. Pate, and G. Scoles, J. Chem. Phys. **100**, 2588 (1994).
30. G. M. Zaslavskii and B. V. Chirikov, UFN **105**, 3 (1971); Sov. Phys. – Usp. **14**, 549 (1972).
31. E. V. Shuryak, ZhETF **71**, 2039 (1976); Sov. Phys. – JETP **44**, 1070 (1976).
32. B. V. Chirikov, Phys. Rep. **52**, 263 (1979).
33. M. V. Kuzmin, V. S. Letokhov, and A. A. Stuchebrukhov, ZhETF **90**, 458 (1986); Sov. Phys. – JETP **63**, 264 (1986).
34. V. N. Bagratashvili, M. V. Kuzmin, V. S. Letokhov, and A. A. Stuchebrukhov, Chem. Phys. **97**, 13 (1985).
35. A. Stuchebrukhov, S. Ionov, and V. Letokhov, J. Phys. Chem. **93**, 5357 (1989).
36. A. A. Makarov, in: Ref. [1], p. 106; p. 177 (in Russian).
37. V. O. Kompanets, V. B. Laptev, A. A. Makarov et al., Pis'ma v ZhETF **92**, 157 (2010); JETP Lett. **92**, 135 (2010).